

Clustering in Globally Coupled Oscillators Near a Hopf Bifurcation: Theory and Experiments

Hiroshi Kori,^{1,2,*} Yoshiki Kuramoto,³ Swati Jain,⁴ István Z. Kiss,⁵ and John Hudson⁴

¹*Department of Information Sciences,*

Ochanomizu University, Tokyo 112-8610, Japan

²*CREST, Japan Science and Technology Agency, Kawaguchi 332-0012, Japan*

³*International Institute for Advanced Studies, Kyoto 619-0225, Japan*

⁴*Department of Chemical Engineering,*

University of Virginia, Charlottesville, Virginia 22904, USA

⁵*Department of Chemistry, Saint Louis University, St. Louis, Missouri 63103, USA*

(Dated: December 3, 2024)

Abstract

A theoretical analysis is presented to show the general occurrence of phase clusters in weakly, globally coupled oscillators close to a Hopf bifurcation. Through a reductive perturbation method, we derive the amplitude equation with a higher order correction term valid near a Hopf bifurcation point. This amplitude equation allows us to calculate analytically the phase coupling function from given limit-cycle oscillator models. Moreover, using the phase coupling function, the stability of phase clusters can be analyzed. We demonstrate our theory with the Brusselator model. Experiments are carried out to confirm the presence of phase clusters close to Hopf bifurcations with electrochemical oscillators.

PACS numbers: 05.45.Xt, 82.40.Bj

*corresponding author: kori.hiroshi@ocha.ac.jp

I. INTRODUCTION

The dynamics of weakly interacting oscillating units can be described with phase models [1]. For example, for N identical oscillators with global (i.e., mean field) coupling, we have

$$\frac{d\phi_i}{dt} = \omega + \frac{\kappa}{N} \sum_{j=1}^N \Gamma(\phi_i - \phi_j), \quad (1)$$

where ϕ_i ($i = 1, \dots, N$) and ω are the phase and the frequency of oscillator i , respectively, κ is the coupling strength, and Γ is the phase coupling function. Phase models have been formulated from ordinary differential equations describing, e.g., chemical reactions [1]. Recently, they have been formulated from direct experiments as well [2–4]. A prominent feature of such phase models is the presence of higher harmonics in the phase coupling function. As a result of higher harmonics, complex dynamics including chaos and multi-phase clusters can be observed [5–9]. Here, we refer to phase clusters as clustering behavior purely attributed to phase dynamics. Clustering dynamics that can not be described by phase models are referred to amplitude clusters [10]. Phase clusters have been experimentally found in a wide range of systems including electrochemical systems, light sensitive BZ reaction, carbon monoxide oxidation on platinum [2, 3, 11–17]. The number of clusters and their appearance with positive or negative coupling/feedback is puzzling. Multi-phase clusters are usually explained by the presence of higher harmonics in the coupling functions in the phase model [5]; however, the mechanism through which higher harmonics can develop is unclear.

In this paper, we give a theoretical explanation for clusters close to oscillations that develop through Hopf bifurcations. With analytical derivation, we show how the higher harmonics occur in the phase coupling function through two-step reductions: an amplitude equation is derived from coupled limit-cycle oscillators through a reductive perturbation method, and then, the phase coupling function is derived from the amplitude equation through the phase reduction method. Experiments are carried out to confirm the presence of multi-phase clusters close to Hopf bifurcations with electrochemical oscillators.

(a)	1 cluster	Desync	Multi-clusters	(b)	1 cluster	Desync	Multi-clusters
$\kappa > 0$	stable	unstable	unstable	$\kappa > 0$	stable	unstable	unstable,
$\kappa < 0$	unstable	neutral	or neutral	$\kappa < 0$	unstable	unstable or neutral	neutral, or stable

TABLE I: (color online) General properties of phase clusters in theoretical models close to a Hopf bifurcation with weak, global coupling. (a) Properties in the lowest order amplitude equation [Eq. (8)]. (b) Properties in the higher order amplitude equation [Eq. (20)]. “Desync” refers to the desynchronized state, which is the state of uniform phase distribution. This state is also called the splay state. Here we assumed that the one cluster state is asymptotically stable for $\kappa > 0$. When one cluster state is stable for $\kappa < 0$, the stability of the desynchronized state is exchanged between $\kappa > 0$ and $\kappa < 0$.

II. THEORY

A. Overview

The Stuart-Landau (SL) oscillator, which is a local element of the complex Ginzburg-Landau model[18, 19], is considered as a general skeleton model for the description of oscillators close to Hopf bifurcations. It can be derived as a lowest-order amplitude equation through a reductive perturbation method [1], as summarized in Sec. II B. However, a population of SL oscillators coupled globally and linearly can not describe multi-phase clusters because its corresponding phase coupling function Γ in Eq. 1 does not contain second and higher harmonics; i.e. $\Gamma(\Delta\phi) \propto \sin(\Delta\phi + \theta) + a_0$, where a_0 and θ are constant [1, 10]. As shown in Table Ia, the stability analysis of such a phase model predicts that the only stable behavior is a one cluster state (in-phase synchrony).

However, it should be noticed that infinitesimally small perturbations given to the Stuart-Landau system may alter a neutral state to a stable or unstable one; i.e., the Stuart-Landau system is structurally unstable. Indeed, we will show that when we take into account higher order correction to the amplitude equation, multi-cluster states may become asymptotically stable. The number of clusters and whether they occur with negative or positive coupling depends on the types of non-linearities in the ordinary differential equations. The stability of the cluster state are weak, nonetheless it is expected that they can be observed in globally

coupled oscillators even very close to Hopf bifurcations.

B. Amplitude equation of the lowest order

Consider a network of identical limit-cycle oscillators with linear coupling

$$\dot{\mathbf{x}}_i = \mathbf{f}(\mathbf{x}_i; \mu) + \mu\kappa \sum_{j=1}^N A_{ij} \hat{D}(\mathbf{x}_j - \mathbf{x}_i), \quad (2)$$

where $\mathbf{x}_i \in \mathbb{R}^m$ is the state variable of the i -th oscillator ($i = 1, \dots, N$), \hat{D} is a $m \times m$ matrix, and $\mu\kappa$ is the coupling strength. We assume $\mathbf{f}(\mathbf{x}; \mu) = 0$ without loss of generality. We also assume that, in the absence of coupling ($\kappa = 0$), the trivial solution $\mathbf{x}_i = 0$ is stable for $\mu < 0$ and undergoes a supercritical Hopf bifurcation at $\mu = 0$, such that each unit becomes a limit-cycle oscillator with the amplitude $\mathbf{x}_i = O(\sqrt{\mu})$ for $\mu > 0$. Hereafter, we consider only $\mu \geq 0$ and put $\mu = \epsilon^2$ for convenience.

To derive the amplitude equation for Eq. (2) near a Hopf bifurcation, it is sufficient to focus on the subsystem in which an oscillator is coupled to another. Let \mathbf{x} and \mathbf{x}' be the state vectors of the oscillators. The dynamical equation for \mathbf{x} is given as

$$\dot{\mathbf{x}} = \mathbf{f}(\mathbf{x}; \epsilon^2) + \epsilon^2 \kappa \hat{D} \mathbf{x}'. \quad (3)$$

We expand $\mathbf{f}(\mathbf{x}; \epsilon^2)$ around $\mathbf{x} = 0$ as

$$\mathbf{f}(\mathbf{x}; \epsilon^2) = \hat{L}_0 \mathbf{x} + \epsilon^2 \hat{L}_1 \mathbf{x} + \mathbf{n}_2(\mathbf{x}, \mathbf{x}) + \mathbf{n}_3(\mathbf{x}, \mathbf{x}, \mathbf{x}) + O(\epsilon^4), \quad (4)$$

where \mathbf{n}_2 and \mathbf{n}_3 are the second and third order terms in the expansion, respectively (their precise definitions are given in Appendix A). Because of the assumption of Hopf bifurcation, \hat{L}_0 has a pair of purely imaginary eigenvalues $\pm i\omega_0$. The right and left eigenvectors of \hat{L}_0 corresponding to the eigenvalue $i\omega_0$ are denoted by \mathbf{u} (column vector) and \mathbf{v} (row vector), respectively; i.e., $\hat{L}_0 \mathbf{u} = \mathbf{v} \hat{L}_0 = i\omega_0 \hat{L}_0$. They are normalized as $\mathbf{v} \mathbf{u} = 1$. The solution to the linearized unperturbed system, $\dot{\mathbf{x}} = \hat{L}_0 \mathbf{x}$, is given by

$$\mathbf{x}_0(t) = w e^{i\theta(t)} \mathbf{u} + \bar{w} e^{-i\theta(t)} \bar{\mathbf{u}}, \quad (5)$$

where w is an arbitrary complex number, which we refer to as the complex amplitude; $\bar{\mathbf{u}}$ and \bar{w} denote the complex conjugate of \mathbf{u} and w , respectively; and $\theta(t) = \omega_0 t$.

In Eq. (2), $\mathbf{x}(t)$ generally deviates from $\mathbf{x}_0(t)$. By interpreting w as a time-dependent variable $w(t)$, it is possible to describe the time-asymptotic behavior of $\mathbf{x}(t)$ in the following form

$$\mathbf{x} = \mathbf{x}_0(w, \bar{w}, \theta) + \boldsymbol{\rho}(w, \bar{w}, w', \bar{w}', \theta), \quad (6)$$

$$\dot{w} = g(w, \bar{w}) + \epsilon^2 \kappa h(w, w', w', \bar{w}'), \quad (7)$$

where $\boldsymbol{\rho}, g$ and h are the functions to be determined perturbatively. Equation (7) is called the amplitude equation. In Ref. 1, the amplitude equation to the lowest order is derived as

$$\dot{w} = \epsilon^2 \alpha w - \beta |w|^2 w + \epsilon^2 \kappa \gamma w', \quad (8)$$

where α, β and γ are the complex constants with the following expressions:

$$\alpha = \mathbf{v} \hat{L}_1 \mathbf{u}, \quad (9)$$

$$\beta = -3\mathbf{v} \mathbf{n}_3(\mathbf{u}, \mathbf{u}, \bar{\mathbf{u}}) + 4\mathbf{v} \mathbf{n}_2(\mathbf{u}, \hat{L}_0^{-1} \mathbf{n}_2(\mathbf{u}, \bar{\mathbf{u}})) + 2\mathbf{v} \mathbf{n}_2(\bar{\mathbf{u}}, (\hat{L}_0 - 2i\omega)^{-1} \mathbf{n}_2(\mathbf{u}, \mathbf{u})), \quad (10)$$

$$\gamma = \mathbf{v} D \mathbf{u}. \quad (11)$$

C. Phase reduction for the the lowest order amplitude equation

Following the method in Ref. 1, we may further reduce the amplitude equation to a phase model. For $\kappa = 0$, Eq. (8) has the stable limit-cycle solution given by

$$w_0(t) = r e^{i\phi(t)} \quad (12)$$

where $r = \epsilon \sqrt{\alpha_R / \beta_R}$ (the subscripts R and I denote the real and imaginary parts, respectively), $\phi(t) = \omega t + \phi_0$, $\omega = \epsilon^2 \alpha_R (c_0 - c_2)$, $c_0 = \alpha_I / \alpha_R$, $c_2 = \beta_I / \beta_R$, and ϕ_0 is an arbitrary initial phase. For sufficiently small κ , the trajectory of $w(t)$ deviates only slightly from that of the unperturbed limit-cycle. In this case, $w(t)$ is well approximated by $r e^{i\phi(t)}$ with the phase $\phi(t)$ obeying the following phase model:

$$\dot{\phi} = \omega + \epsilon^2 \kappa \Gamma(\phi - \phi'). \quad (13)$$

The phase coupling function Γ is obtained through

$$\Gamma(\phi - \phi') = \langle z(\phi) \cdot h(w_0, w'_0) \rangle, \quad (14)$$

where $z(\phi)$ is the phase sensitivity function, $a \cdot b = (\bar{a}b + a\bar{b})/2$ denotes the inner product in a complex form, and $\langle f(\phi, \phi') \rangle = \frac{1}{2\pi} \int_0^{2\pi} f(\phi + \mu, \phi' + \mu) d\mu$ denotes averaging. The phase sensitivity function is determined by the nature of limit-cycle oscillation. In the case of Eq. (8), we have [1]

$$z(\phi) = \frac{-c_2 + i}{r} e^{i\phi}. \quad (15)$$

For convenience, we expand the phase coupling function Γ as

$$\Gamma(\psi) = a_0 + \sum_{\ell=1}^{\infty} (a_{\ell} \cos \ell\psi + b_{\ell} \sin \ell\psi). \quad (16)$$

Substituting Eq. (15) and $h(w_0, w'_0) = \gamma w'_0 = \gamma r e^{i\phi'}$ to Eq. (14), we find

$$a_1 = \gamma_R (c_1 - c_2), \quad (17)$$

$$b_1 = -\gamma_R (1 + c_1 c_2), \quad (18)$$

where $c_1 \equiv \gamma_I/\gamma_R$. Importantly, all other coefficients vanish.

Note that, if the coupling term in Eq. (3) is diffusive [i.e., $\epsilon^2 \kappa \hat{D}(\mathbf{x}' - \mathbf{x})$ instead of $\epsilon^2 \kappa \hat{D}\mathbf{x}'$], we have $h(w_0, w'_0) = \gamma(w'_0 - w_0)$. In this case, we obtain $a_0 = -a_1$ in addition to Eqs. (17) and (18).

We have seen that, for the lowest order amplitude equation given by Eq. (8), the corresponding phase coupling function does not contain the second and higher harmonics. Therefore, as briefly mentioned in Sec. II A, this amplitude equation does not admit multi-phase clusters.

D. Higher order correction

Now, we derive higher order correction terms to the amplitude equation and the corresponding phase coupling function Γ .

At first, we discuss higher order terms in $g(w)$ in Eq. (7). We know that $g(w)$ consists only of $|w|^n w$ ($n = 0, 1, 2, \dots$), called the resonant terms [20]. The dynamical equation $\dot{w} = g(w)$ is invariant under the transformation $w \rightarrow w e^{i\phi}$; i.e., the system has the rotational symmetry. This implies that $w_0(\phi)$ and $z(\phi)$ have the following forms: $w_0(\phi) = w_0(0) e^{i\phi}$ and $z(\phi) = z(0) e^{i\phi}$. Then, obviously, $\Gamma(\phi - \phi') = \langle z(\phi) \cdot \gamma w'_0(\phi') \rangle$ still contains only the first harmonics.

Therefore, for Γ to possess higher harmonics, we need to consider higher order correction to $h(w, w')$. Note that $h(w, w')$ is a polynomial of w, \bar{w}, w', \bar{w}' in general; i.e., $h(w, w') = w^{\ell_1} \bar{w}^{\ell_2} w'^{\ell_3} \bar{w}'^{\ell_4}$ with integers $\ell_1, \ell_2, \ell_3, \ell_4 \geq 0$. Because $w_0 = O(\epsilon)$ and $z = O(\epsilon^{-1})$ [see Eqs. (12) and (15)], we have $z \cdot h = O(\epsilon^{\ell_1 + \ell_2 + \ell_3 + \ell_4 - 1})$. We also have $z \cdot h(w, w') \propto e^{i(\ell_1 - \ell_2 - 1)\phi} e^{i(\ell_3 - \ell_4)\phi'}$. This term contributes to a_ℓ and b_ℓ ($\ell > 0$) when this term is a function of only $\pm\ell(\phi - \phi')$; i.e., $\ell_1 - \ell_2 - 1 = \pm\ell$ and $\ell_3 - \ell_4 = \mp\ell$. Obviously, $\bar{w}^{\ell-1} w'^\ell = O(\epsilon^{2(\ell-1)})$ gives a leading contribution to a_ℓ and b_ℓ . We thus find

$$a_\ell, b_\ell = O(\epsilon^{2(\ell-1)}). \quad (19)$$

Other terms in $h(w, w')$ together with higher order terms in $g(w)$ provide minor corrections to the coefficients a_ℓ and b_ℓ . As discussed in Sec. III A, the stability of phase clusters crucially depends on the magnitude of these coefficients.

Hence, as a second order description of the amplitude equation, it is appropriate to consider

$$\dot{w} = \epsilon^2 \alpha w - \beta |w|^2 w + \epsilon^2 \kappa (\gamma w' + \delta \bar{w}^2 w'), \quad (20)$$

with complex constant δ . One of the main results in the present paper is, as shown in Appendix A, the derivation of the expression for δ , which has the following concise expression:

$$\delta = 2\mathbf{v}\mathbf{n}_2(\bar{\mathbf{u}}, (\hat{L}_0 - 2i\omega)^{-1} D(\hat{L}_0 - 2i\omega)^{-1} \mathbf{n}_2(\mathbf{u}, \mathbf{u})). \quad (21)$$

Moreover, calculation of $\langle z(\phi), \delta \bar{w}_0^2(\phi) w'_0(\phi') \rangle$ yields the Fourier coefficients of Γ , given as

$$a_2 = r^2 \delta_R (c_3 - c_2), \quad (22)$$

$$b_2 = -r^2 \delta_R (1 + c_2 c_3), \quad (23)$$

where $c_3 = \delta_I / \delta_R$.

III. DEMONSTRATION

Our theory is applied to the prediction of cluster states in globally coupled oscillators. First, we briefly summarize the existence and stability of cluster states in the phase model with global coupling. We then numerically confirm our prediction about clustering behavior in the Brusselator model.

A. Existence and stability of balanced cluster states

A globally coupled system with N oscillators is obtained by replacing \mathbf{x}' in Eq. (3) with $\mathbf{X} \equiv \frac{1}{N} \sum_{j=1}^N \mathbf{x}_j$. The corresponding phase model is given in Eq. (1), where we put $\epsilon^2 = 1$ without loss of generality. Because all the eigenvalues obtained below will be just proportional to κ and there is no other κ -dependence, we put $\kappa = 1$ for simplicity.

The balanced n -cluster state ($n \geq 2$) is the state in which the whole population splits into equally populated n groups (here we assume that N is a multiple of n), oscillators in group m ($m = 0, 1, \dots, n$) have an identical phase ψ_m , and the phase of groups are equally separated ($\psi_m = \Omega t + 2m\pi/n$). In Eq. (1), this solution always exist for any n .

The stability of the balanced cluster states was studied by Okuda [5]. The n -cluster state with $n \geq 2$ possesses two types of eigenvalues, which are associated with intra-cluster and inter-cluster perturbations. The eigenvalue associated with intra-cluster perturbations is given by $\lambda_n^{\text{intra}} = \sum_{k=1}^{\infty} b_{kn}$. Therefore, in the absence of the ℓ -th harmonics with $\ell \geq n$ in Γ , the n -cluster state has a zero eigenvalue. That is, the n -cluster state may not be asymptotically stable. This is the reason why any multi-phase clusters do not appear in the lowest order amplitude equation given by Eq. (8). Note that, however, strong coupling may cause a different type of cluster states called amplitude cluster [10].

As discussed in Sec. IID, higher order correction to the amplitude equation yields Eq. (19). We thus have $\lambda_n^{\text{intra}} = \sum_{k=1}^{\infty} b_{kn} = O(\epsilon^{2n-1})$, implying that multi-phase clusters can be asymptotically stable. This estimation also implies that n -cluster states with larger n can be more stabilized for larger ϵ^2 . Therefore, more phase clusters are likely to appear as the system is farther from the Hopf bifurcation point.

From here, we focus on one and two cluster states. When we neglect third and higher harmonics in Γ , eigenvalues for one and two cluster states are given by

$$\lambda_1^{\text{intra}} = \Gamma'(0) = b_1 + 2b_2, \quad (24)$$

$$\lambda_2^{\text{intra}} = \frac{1}{2} (\Gamma'(0) + \Gamma(\pi)) = 2b_2, \quad (25)$$

$$\lambda_2^{\text{inter}} = \Gamma'(\pi) = -b_1 + 2b_2. \quad (26)$$

Moreover, there exists a family of two cluster states with the phase difference between the clusters being different from π . These cluster states often show interesting dynamical behavior called slow switching [6–8]. Although the clusters are generally not equally populated, we

consider only two equally populated clusters for simplicity. For this cluster state, one may show that the phase difference $\Delta\phi$ between the clusters is given by $\Delta\phi = \arccos(-b_1/2b_2)$. Because $b_2 = O(\epsilon)$, the solution to $\Delta\phi$ exists only when b_1 is of $O(\epsilon)$ or even smaller. Because $\lambda_1^{\text{intra}} = O(\epsilon)$ in this case, this situation is expected to occur near the stability boundary for the one cluster state ($\lambda_1^{\text{intra}} = 0$).

There are three types of eigenvalues for this two cluster state, given as

$$\lambda_{\text{ss}}^1 = \frac{1}{2} (\Gamma'(0) + \Gamma'(\Delta\phi)) = -a_1 \sin \Delta\phi + O(\epsilon), \quad (27)$$

$$\lambda_{\text{ss}}^2 = \frac{1}{2} (\Gamma'(0) + \Gamma'(-\Delta\phi)) = a_1 \sin \Delta\phi + O(\epsilon), \quad (28)$$

$$\lambda_{\text{ss}}^3 = \frac{1}{2} (\Gamma'(\Delta\phi) + \Gamma'(-\Delta\phi)) = \frac{(b_1 + 2b_2)(b_1 - 2b_2)}{b_2}. \quad (29)$$

The slow switching dynamics appear [6, 7] when $\lambda_{\text{ss}}^1 \lambda_{\text{ss}}^2 < 0$, $\lambda_{\text{ss}}^3 < 0$, and

$$\lambda_{\text{ss}}^1 + \lambda_{\text{ss}}^2 = \frac{b_1(b_1 + 2b_2)}{b_2} < 0. \quad (30)$$

As a_1 is generally of $O(1)$, the first condition always holds true, while the rest conditions depend on b_1 and b_2 values.

We summarize general properties of the cluster states. The stability of one and two balanced cluster states can be computed by Eqs. (24)–(26). Slow switching dynamics typically appear near the stability boundary of the one cluster state. As ϵ increases, balanced cluster states with large number of clusters are more likely to appear.

B. Numerical verification with limit-cycle oscillators

To demonstrate our theory, we consider a population of Brusselator oscillators with global coupling, whose dynamical equations are given by

$$\frac{dx_i}{dt} = A - (B + 1)x_i + x_i^2 y_i + \frac{\kappa}{N} \sum_{j=1}^N (x_j - x_i), \quad (31a)$$

$$\frac{dy_i}{dt} = Bx_i - x_i^2 y_i + \frac{\kappa d}{N} \sum_{j=1}^N (y_j - y_i). \quad (31b)$$

We consider B as a control parameter, while fixing other parameters A and d . In the absence of coupling (i.e., $\kappa = 0$), the Hopf bifurcation occurs at $B = B_c \equiv 1 + A^2$. The bifurcation parameter is defined as $\epsilon^2 = \frac{B - B_c}{B_c}$ for $B > B_c$. As shown in Appendix B,

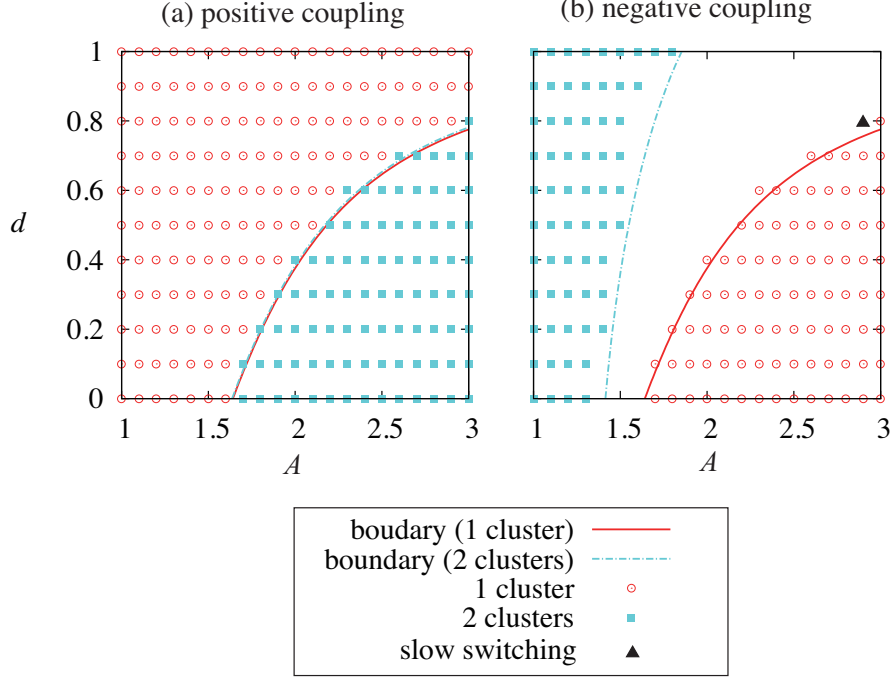


FIG. 1: (color online) Phase diagram of cluster states in the Brusselator system. Lines show stability boundaries obtained via Eqs. (24)–(29). Numerical data is obtained by direct numerical simulations of Eqs. (31a) and (31b) with $N = 4$, $B = (1 + \epsilon^2)B_c$, $\epsilon = r^2(2 + A^2)/(A^2(1 + A^2))$, $r = 0.01$, (a) $\kappa = 0.001$, (b) $\kappa = -0.001$.

using the expressions given in Sec. II, we obtained Fourier coefficients a_1, a_2, b_1 and b_2 of Γ as functions of A, B, d and ϵ . Substituting them into Eqs. (24)–(26), we obtained the stability boundaries of the cluster states in the parameter space. Figure 1 displays the phase diagram in the parameter space (A, d) , where the lines show the predicted stability boundaries. Moreover, we also calculated the eigenvalues for the slow switching state, given by Eqs. (27)–(29), and found that it exists and is stable near the stability boundary of the one cluster state for $\kappa < 0$.

We carried out direct numerical simulations of Eqs. (31a) and (31b). Starting from random initial conditions, the system typically converged to balanced cluster states. Some snapshots are displayed in Fig. 2. The symbols in Fig. 1 display the parameter sets at which the indicated cluster state is obtained. We also found the slow switching dynamics at the filled triangle in Fig. 1(b)], as theoretically expected. All together, we see an excellent agreement between the analytical and numerical results.

We next observed clustering behavior for various B values far from the bifurcation point

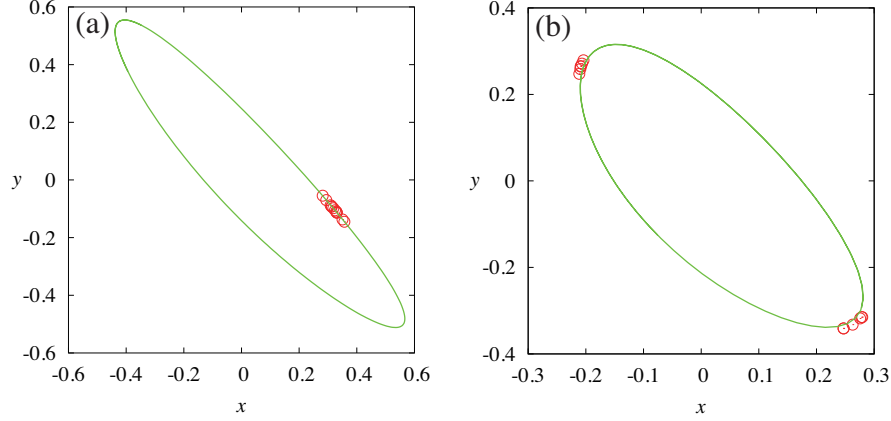


FIG. 2: (color online) Snapshots of cluster states in the Brusselator system. For a better presentation, displayed snapshots are those before complete convergence. Parameter values: $\kappa = -0.001, d = 0.4, B = (1 + \epsilon^2)B_c, \epsilon = r^2(2 + A^2)/(A^2(1 + A^2)), r = 0.01$, (a) $A = 2.8$, (b) $A = 1.1$.

B_c with $N = 24$ oscillators. We fixed $A = 1.0$, so that $B_c = 2.0$. At each B value, we employed 100 different random initial conditions. For each initial condition, we checked the number of phase clusters after transient time. Figure 3 shows how many times the n cluster state was obtained for each B value. As the system is farther from the bifurcation point, n cluster states with larger n values were obtained. In this particular case, the number of clusters tends to increase as the system is farther from the bifurcation point, which is consistent with our theoretical prediction.

IV. EXPERIMENTS

Experiments were conducted with a population of nearly identical $N = 64$ electrochemical oscillators. Each oscillator is represented by a 1 mm diameter Ni wire embedded in epoxy and immersed in 3 mol/L sulfuric acid. The oscillators exhibit smooth or relaxation waveforms for the current (the rate of dissolution), depending on the applied potential (V) vs. a Hg/Hg₂SO₄/cc. K₂SO₄ reference electrode. The current of the electrodes became oscillatory through a supercritical Hopf bifurcation point at $V = 1.0$ V; the oscillations are smooth near the Hopf bifurcation point. As the potential is increased, relaxation oscillations are seen that disappear into a steady state through a homoclinic bifurcation at about $V = 1.31$ V [21]. The parameters (applied potential) were chosen such that the oscillators exhibit

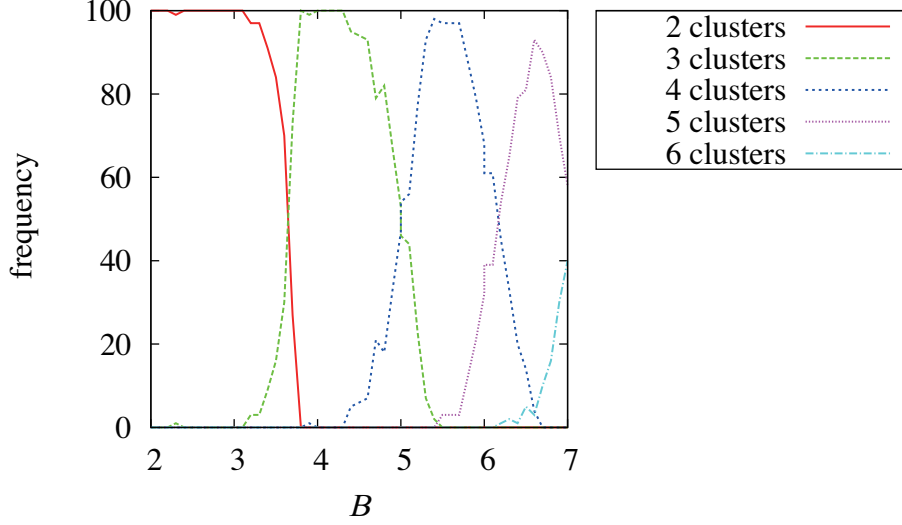


FIG. 3: (color online) Clustering behavior in the Brusselator system farther from the Hopf bifurcation point. Each line indicates how many times the n cluster state was obtained out of 100 different initial conditions. $N = 24$, $A = 1.0$, $d = 0.7$, $\kappa = -0.01$. Initial values of x_i and y_i are random numbers taken from the uniform distribution in the range $[-0.05, 0.05]$.

smooth oscillations near the Hopf bifurcation without any coupling. The electrodes were then coupled with a combination of series (R_s) and parallel (R_p) resistors such that the total resistance $R_{tot} = R_p + 64R_s$ is kept constant at 652 Ohm. The imposed coupling strength can be computed as $K = NR_s/R_p$ (More experimental details are given in Ref. [22]). Negative coupling was induced with the application of negative series resistance supplied by a PAR 273A potentiostat in the form of IR compensation).

Three cluster states were observed near the Hopf bifurcation ($V = 1.05$ V) with negative coupling. Fig. 4(a) shows the current from one oscillator of each of the three clusters. The configuration of these clusters is shown on a grid of 8 x 8 circles. Each color or shade represents one cluster. In the previous work on the same system it had been shown that with positive coupling close to the Hopf bifurcation only one-cluster state is present [2]. Phase response curves (Fig. 4(c)) and coupling functions (Fig. 4(d)) for these oscillators were determined experimentally by introducing slight perturbations to the oscillations [2]. The stability of these cluster states was determined by computing the eigenvalues of the phase model [5]. The maxima of real parts of these eigenvalues, for the same potential as in Fig. 4(a), are shown in Fig. 4(e). It is clear that with negative coupling multi-cluster states

should be observed (Fig. 4(a)) and the three-cluster state is the most stable state.

As the potential was varied the number of cluster states changed. Four and five cluster states were observed at higher potentials. Examples of the oscillation waveforms and configurations for the 4 and 5 cluster states are shown in Figs. 5(a), (b), (c), and (d). Further increase in the potential resulted in complete desynchronization of the 64 oscillators. At higher potentials, for moderately relaxational oscillators, only one cluster state was observed. Fig. 5(e) summarizes the effect of changing the parameter (potential) on the existence of different cluster states. The presence of these clusters can be explained by the most stable clusters from the experimentally determined phase model (Fig. 5(f)). (We were not able to derive a phase model for the two-cluster state because the amplitude of the oscillations was too small for response functions to be measured in experiments.)

The experiments thus confirm that varying number of clusters (2-5) can be observed in the electrochemical system close to Hopf bifurcation with negative global coupling. Note that these clusters are different than those reported previously that had been obtained with relaxation oscillators with positive coupling [22]. Similar to the results obtained with the Brusselator model, when the system is shifted farther away from the Hopf bifurcation, the number of clustered increased due to the emergence of stronger higher harmonics in the coupling function. In agreement with the theory, the clusters required relatively strong negative coupling ($K \approx -0.88$) in contrast with the one cluster state with positive coupling that required very weak coupling ($K < 0.05$) [23]. Therefore, we see that weak higher harmonics can play important role in determining the dynamical features of cluster formation when the contribution of dominant harmonics does not induce a stable structure.

V. CONCLUDING REMARKS

In summary, we have shown theoretically and confirmed numerically and experimentally the development of higher harmonics in the phase coupling function and the appearance of phase clusters in globally coupled oscillatory systems. We found that the only relevant higher-order terms that should be included in the amplitude equation are $\bar{w}^{\ell-1}w'^{\ell}$ with $\ell \geq 2$. In particular, we derived the expression for the coefficient of the term \bar{w}^2w' , which has, to our surprise, a very concise form. The relevance of higher harmonics in the phase coupling function has been well recognized. Our study uncovered how higher harmonics

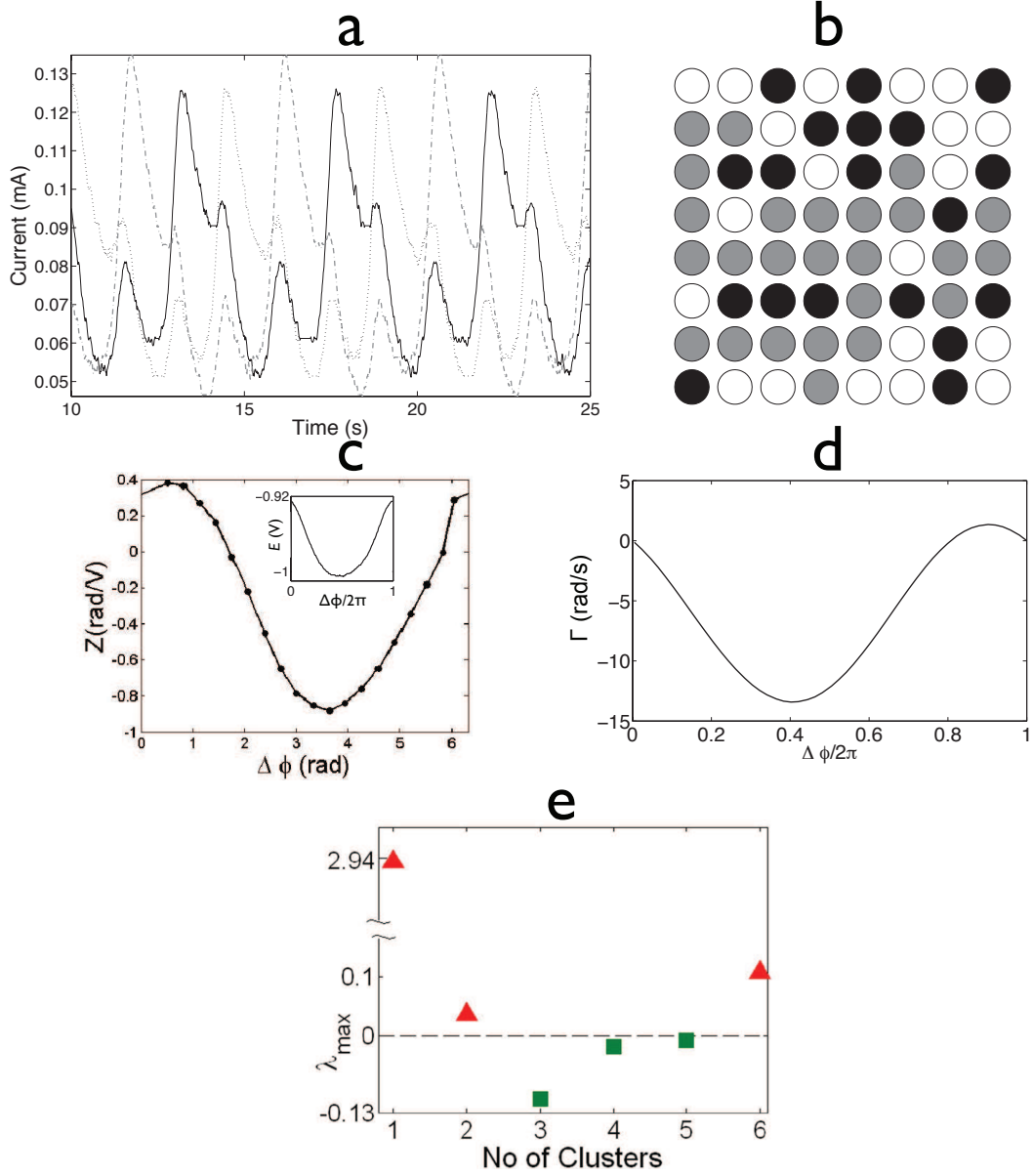


FIG. 4: (color online) Experiments: Three cluster state close to Hopf-bifurcation with negative global coupling of sixty-four electrochemical oscillators. $K = -0.88$ (a) Current time series and the three cluster configuration at $V = 1.05$ V (close to a Hopf bifurcation.) Solid, dashed, and dotted curves represent currents from the three clusters. b) Cluster configuration. (White, black, and grey circles represent the three clusters.) (c) Response function and waveform (inset) of electrode potential $E = V - IR_{tot}$, where I is the current of the single oscillator. d) Phase coupling function. e) Stability analysis of the clusters with experiment-based phase models for $K = -1$: the maximum of the real parts of eigenvalues vs. the number of (balanced) cluster states.

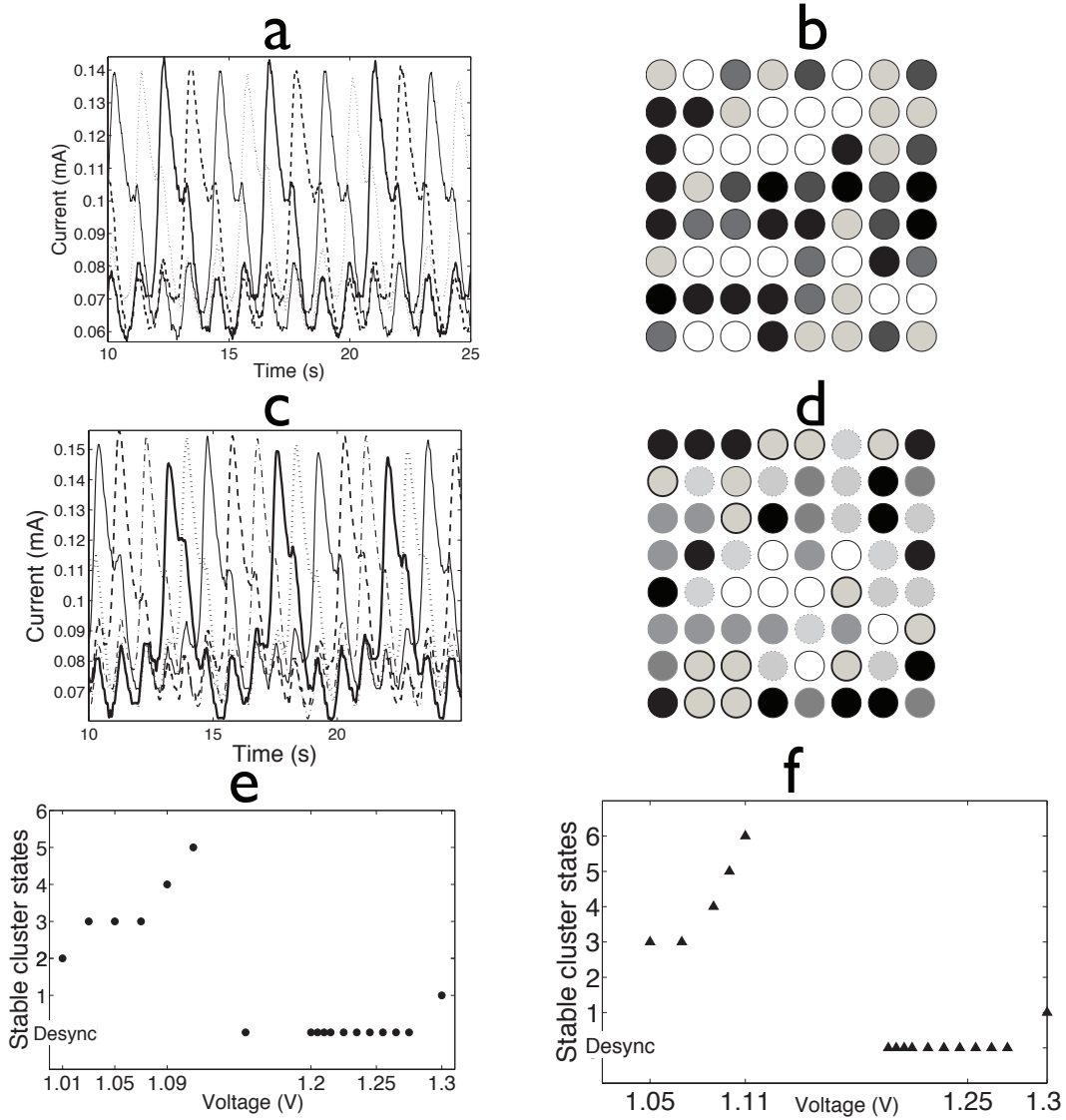


FIG. 5: Experiments: Multiple cluster states observed as the parameters are moved away from Hopf-bifurcation with negative global coupling for sixty-four electrochemical oscillators. Top row: four clusters, $V = 1.09V$, $K = -0.88$. Middle row: five clusters. $V = 1.11V$, $K = -0.88$ (a) Current time series of the four clusters. (b) Cluster configuration (17:14:15:18) for four cluster state. (c) Current time series. (d) Cluster configuration (15:13:14:7:15) of five cluster state. (e) Experimentally observed cluster states as a function of applied potential. (f) Stable cluster state as a function of potential predicted by the experimentally obtained phase model.

are developed in limit-cycle oscillators near a Hopf bifurcation point. We also expect that the derived amplitude equation will serve as an analytically tractable limit-cycle oscillator model that produces higher harmonics in the phase coupling function.

Appendix A: Derivation of the amplitude equation

Our aim is to reduce Eq. (3) to the amplitude equation given by Eq. (20). Because the expressions for α, β and γ are obtained in Ref. 1, we focus on δ .

For convenience, we rewrite Eq. (3) and Eq. (7) as

$$\dot{\mathbf{x}} = \hat{L}_0 \mathbf{x} + \epsilon^2 \hat{L}_1 \mathbf{x} + \mathbf{n}_2(\mathbf{x}, \mathbf{x}) + \mathbf{n}_3(\mathbf{x}, \mathbf{x}, \mathbf{x}) + \epsilon^2 \kappa \hat{D} \mathbf{x}', \quad (\text{A1})$$

$$\dot{w} = G(w, \bar{w}, w', \bar{w}'), \quad (\text{A2})$$

respectively. Here, \mathbf{n}_2 and \mathbf{n}_3 are defined as

$$\mathbf{n}_2(\mathbf{u}, \mathbf{v}) = \sum_{i,j=1}^M \frac{1}{2!} \left(\frac{\partial^2 \mathbf{f}}{\partial x_i \partial x_j} \right)_{\mathbf{x}=0} u_i v_j, \quad (\text{A3})$$

$$\mathbf{n}_3(\mathbf{u}, \mathbf{v}, \mathbf{w}) = \sum_{i,j,k=1}^M \frac{1}{3!} \left(\frac{\partial^3 \mathbf{f}}{\partial x_i \partial x_j \partial x_k} \right)_{\mathbf{x}=0} u_i v_j w_k. \quad (\text{A4})$$

Note that we consider only linear coupling in Eq. (A1). If nonlinear coupling terms is added to Eq. (A1), the expression for δ will be different from Eq. (21) while α, β and γ are unchanged.

By substituting Eq. (6) into Eq. (A1) and using Eq. (A2), we obtain

$$\mathcal{L}_0 \boldsymbol{\rho} = G \exp(i\theta) \mathbf{u} + \bar{G} \exp(-i\theta) \bar{\mathbf{u}} + \mathbf{b}(w, \bar{w}, w', \bar{w}', \theta), \quad (\text{A5})$$

where

$$\mathcal{L}_0 = \hat{L}_0 - \omega_0 \frac{\partial}{\partial \theta}, \quad (\text{A6})$$

$$\begin{aligned} \mathbf{b} = & -\epsilon^2 \hat{L}_1 \mathbf{x} - \mathbf{n}_2(\mathbf{x}, \mathbf{x}) - \mathbf{n}_3(\mathbf{x}, \mathbf{x}, \mathbf{x}) - \epsilon^2 \kappa \hat{D} \mathbf{x}' \\ & + G \frac{\partial \boldsymbol{\rho}}{\partial w} + \bar{G} \frac{\partial \boldsymbol{\rho}}{\partial \bar{w}} + G' \frac{\partial \boldsymbol{\rho}}{\partial w'} + \bar{G}' \frac{\partial \boldsymbol{\rho}}{\partial \bar{w}'}. \end{aligned} \quad (\text{A7})$$

Regard Eq. (A5) formally as an inhomogeneous linear differential equation for $\boldsymbol{\rho}(\theta)$, where the right-hand side as a whole represents the inhomogeneous term. To solve Eq. (A5), $\boldsymbol{\rho}(\theta)$ and $\mathbf{b}(\theta)$ are expanded as

$$\boldsymbol{\rho}(\theta) = \sum_{\ell=-\infty}^{\infty} \boldsymbol{\rho}^{(\ell)} \exp(i\ell\theta), \quad (\text{A8})$$

$$\mathbf{b}(\theta) = \sum_{\ell=-\infty}^{\infty} \mathbf{b}^{(\ell)} \exp(i\ell\theta). \quad (\text{A9})$$

Note that the terms $\exp(i\theta)\mathbf{u}$ and its complex conjugate in Eq. (A5) are the zero-eigenvectors of \mathcal{L}_0 ; i.e., $\mathcal{L}_0(e^{i\theta}\mathbf{u}) = \mathcal{L}_0(e^{-i\theta}\bar{\mathbf{u}}) = 0$. Because the left-hand side in Eq. (A5) is free of the zero-eigenvector components due to the operation of \mathcal{L}_0 , these components must be canceled in the right-hand side as well. This condition is called the solvability condition. By substituting Eqs. (A8) and (A9) into Eq. (A5), and comparing the component of $\exp(i\theta)$ in both sides, we obtain the solvability condition $G\mathbf{u} = \mathbf{b}^{(1)}$, or

$$G = -\mathbf{v}\mathbf{b}^{(1)}. \quad (\text{A10})$$

Further, by comparing other components, we obtain

$$\boldsymbol{\rho}^{(\ell)} = (\hat{L}_0 - i\ell\omega_0)^{-1}\mathbf{b}^{(\ell)}, \quad (\ell \neq \pm 1), \quad (\text{A11})$$

$$\boldsymbol{\rho}^{(1)} = (\hat{L}_0 - i\omega_0)^{-1}(\mathbf{b}^{(1)} - G\mathbf{u}), \quad (\text{A12})$$

$$\boldsymbol{\rho}^{(-1)} = (\hat{L}_0 + i\omega_0)^{-1}(\mathbf{b}^{(-1)} - \bar{G}\bar{\mathbf{u}}). \quad (\text{A13})$$

Let $\mathbf{b}^{(\ell)}$ and $\boldsymbol{\rho}^{(\ell)}$ be further expanded in the powers of ϵ :

$$\mathbf{b}^{(\ell)} = \sum_{\nu=2}^{\infty} \epsilon^{\nu} \mathbf{b}_{\nu}^{(\ell)}, \quad (\text{A14})$$

$$\boldsymbol{\rho}^{(\ell)} = \sum_{\nu=2}^{\infty} \epsilon^{\nu} \boldsymbol{\rho}_{\nu}^{(\ell)}. \quad (\text{A15})$$

Correspondingly, \mathbf{b} and $\boldsymbol{\rho}$ themselves are expanded as

$$\mathbf{b} = \sum_{\nu=2}^{\infty} \epsilon^{\nu} \mathbf{b}_{\nu}, \quad (\text{A16})$$

$$\boldsymbol{\rho} = \sum_{\nu=2}^{\infty} \epsilon^{\nu} \boldsymbol{\rho}_{\nu}. \quad (\text{A17})$$

Let G be also expanded as

$$G = \sum_{\nu=1}^{\infty} \epsilon^{2\nu+1} G_{2\nu+1}, \quad (\text{A18})$$

where we have anticipated the absence of even powers.

To derive Eq. (20), we need to calculate G_3 and G_5 . As G_3 is already obtained in Ref. 1, our main concern is G_5 , especially the higher order coupling term in G_5 . To obtain G_3 and G_5 , we need the expressions for \mathbf{b}_{ν} ($\nu = 1, \dots, 5$). Because $\mathbf{x}_0 = O(\epsilon)$; $\mathbf{b}_{\nu}, \boldsymbol{\rho}_{\nu} = O(\epsilon^{\nu})$

($\nu \geq 2$); $G_\nu = O(\epsilon^\nu)$ ($\nu \geq 3$), we find

$$\mathbf{b}_2 = -\mathbf{n}_2(\mathbf{x}_0, \mathbf{x}_0), \quad (\text{A19})$$

$$\mathbf{b}_3 = -\epsilon^2 \hat{L}_1 \mathbf{x}_0 - 2\mathbf{n}_2(\mathbf{x}_0, \boldsymbol{\rho}_2) - \mathbf{n}_3(\mathbf{x}_0, \mathbf{x}_0, \mathbf{x}_0) - \kappa \epsilon^2 \hat{D} \mathbf{x}'_0, \quad (\text{A20})$$

$$\begin{aligned} \mathbf{b}_4 = & -\epsilon^2 \hat{L}_1 \boldsymbol{\rho}_2 - 2\mathbf{n}_2(\mathbf{x}_0, \boldsymbol{\rho}_3) - \mathbf{n}_2(\boldsymbol{\rho}_2, \boldsymbol{\rho}_2) \\ & - 3\mathbf{n}_3(\mathbf{x}_0, \mathbf{x}_0, \boldsymbol{\rho}_2) - \kappa \epsilon^2 \hat{D} \boldsymbol{\rho}'_2, \end{aligned} \quad (\text{A21})$$

$$\begin{aligned} \mathbf{b}_5 = & -\epsilon^2 \hat{L}_1 \boldsymbol{\rho}_3 - 2\mathbf{n}_2(\mathbf{x}_0, \boldsymbol{\rho}_4) - 2\mathbf{n}_2(\boldsymbol{\rho}_2, \boldsymbol{\rho}_3) \\ & - 3\mathbf{n}_3(\mathbf{x}_0, \mathbf{x}_0, \boldsymbol{\rho}_3) - 3\mathbf{n}_3(\mathbf{x}_0, \boldsymbol{\rho}_2, \boldsymbol{\rho}_2) - \kappa \epsilon^2 \hat{D} \boldsymbol{\rho}'_3 \\ & + G_3 \frac{\partial \boldsymbol{\rho}_2}{\partial w} + \bar{G}_3 \frac{\partial \boldsymbol{\rho}_2}{\partial \bar{w}} + G'_3 \frac{\partial \boldsymbol{\rho}_2}{\partial w'} + \bar{G}'_3 \frac{\partial \boldsymbol{\rho}_2}{\partial \bar{w}'}. \end{aligned} \quad (\text{A22})$$

We first calculate $G_3 = \mathbf{v} \mathbf{b}_3^{(1)}$. Using

$$\begin{aligned} \mathbf{b}_3^{(1)} = & -\epsilon^2 \hat{L}_1 \mathbf{x}_0^{(1)} - 2\mathbf{n}_2(\mathbf{x}_0, \boldsymbol{\rho}_2)^{(1)} - \mathbf{n}_3(\mathbf{x}_0, \mathbf{x}_0, \mathbf{x}_0)^{(1)} \\ = & -\epsilon^2 \hat{L}_1 \mathbf{x}_0^{(1)} - 2\mathbf{n}_2(\mathbf{x}_0^{(1)}, \boldsymbol{\rho}_2^{(0)}) - 2\mathbf{n}_2(\mathbf{x}_0^{(-1)}, \boldsymbol{\rho}_2^{(2)}) \\ & - 3\mathbf{n}_3(\mathbf{x}_0^{(1)}, \mathbf{x}_0^{(1)}, \mathbf{x}_0^{(-1)}) - \kappa \epsilon^2 \hat{D} \mathbf{x}_0'^{(1)}, \end{aligned} \quad (\text{A23})$$

$$\begin{aligned} \boldsymbol{\rho}_2^{(0)} = & -\hat{L}_0^{-1} \mathbf{b}_2^{(0)} \\ = & -2\hat{L}_0^{-1} \mathbf{n}_2(\mathbf{x}_0^{(1)}, \mathbf{x}_0^{(-1)}) \end{aligned} \quad (\text{A24})$$

$$\begin{aligned} \boldsymbol{\rho}_2^{(2)} = & (\hat{L}_0 - 2i\omega_0)^{-1} \mathbf{b}_2^{(2)} \\ = & (\hat{L}_0 - 2i\omega_0)^{-1} \mathbf{n}_2(\mathbf{x}_0^{(1)}, \mathbf{x}_0^{(1)}) \end{aligned} \quad (\text{A25})$$

we obtain Eq. (8) with Eqs. (9)–(11).

Now we consider $G_5 = \mathbf{v}\mathbf{b}_5^{(1)}$. We have

$$\begin{aligned}
\mathbf{b}_5^{(1)} &= -\epsilon^2 \hat{L}_1 \boldsymbol{\rho}_3^{(1)} - 2\mathbf{n}_2(\mathbf{x}_0, \boldsymbol{\rho}_4)^{(1)} - 2\mathbf{n}_2(\boldsymbol{\rho}_2, \boldsymbol{\rho}_3)^{(1)} \\
&\quad - 3\mathbf{n}_3(\mathbf{x}_0, \mathbf{x}_0, \boldsymbol{\rho}_3)^{(1)} - 3\mathbf{n}_3(\mathbf{x}_0, \boldsymbol{\rho}_2, \boldsymbol{\rho}_2)^{(1)} - \kappa\epsilon^2 \hat{D}\boldsymbol{\rho}_3'^{(1)} \\
&\quad + G_3 \frac{\partial \boldsymbol{\rho}_2^{(1)}}{\partial w} + \bar{G}_3 \frac{\partial \boldsymbol{\rho}_2^{(1)}}{\partial \bar{w}} + G_3' \frac{\partial \boldsymbol{\rho}_2^{(1)}}{\partial w'} + \bar{G}_3' \frac{\partial \boldsymbol{\rho}_2^{(1)}}{\partial \bar{w}'} \\
&= -\epsilon^2 \hat{L}_1 \boldsymbol{\rho}_3^{(1)} - \mathbf{n}_2(\mathbf{x}_0^{(1)}, \boldsymbol{\rho}_4^{(0)}) - 2\mathbf{n}_2(\mathbf{x}_0^{(-1)}, \boldsymbol{\rho}_4^{(2)}) \\
&\quad - 2\mathbf{n}_2(\boldsymbol{\rho}_2^{(0)}, \boldsymbol{\rho}_3^{(1)}) - 2\mathbf{n}_2(\boldsymbol{\rho}_2^{(2)}, \boldsymbol{\rho}_3^{(-1)}) - 2\mathbf{n}_2(\boldsymbol{\rho}_2^{(-2)}, \boldsymbol{\rho}_3^{(3)}) \\
&\quad - 3\mathbf{n}_3(\mathbf{x}_0^{(1)}, \mathbf{x}_0^{(1)}, \boldsymbol{\rho}_3^{(-1)}) - 6\mathbf{n}_3(\mathbf{x}_0^{(1)}, \mathbf{x}_0^{(-1)}, \boldsymbol{\rho}_3^{(1)}) \\
&\quad - 3\mathbf{n}_3(\mathbf{x}_0^{(-1)}, \mathbf{x}_0^{(-1)}, \boldsymbol{\rho}_3^{(3)}) - 3\mathbf{n}_3(\mathbf{x}_0^{(1)}, \boldsymbol{\rho}_2^{(0)}, \boldsymbol{\rho}_2^{(0)}) \\
&\quad - 6\mathbf{n}_3(\mathbf{x}_0^{(-1)}, \boldsymbol{\rho}_2^{(0)}, \boldsymbol{\rho}_2^{(2)}) - 6\mathbf{n}_3(\mathbf{x}_0^{(-1)}, \boldsymbol{\rho}_2^{(2)}, \boldsymbol{\rho}_2^{(0)}) \\
&\quad - \kappa\epsilon^2 \hat{D}\boldsymbol{\rho}_3'^{(1)} \\
&\quad + G_3 \frac{\partial \boldsymbol{\rho}_2^{(1)}}{\partial w} + \bar{G}_3 \frac{\partial \boldsymbol{\rho}_2^{(1)}}{\partial \bar{w}} + G_3' \frac{\partial \boldsymbol{\rho}_2^{(1)}}{\partial w'} + \bar{G}_3' \frac{\partial \boldsymbol{\rho}_2^{(1)}}{\partial \bar{w}'}
\end{aligned} \tag{A26}$$

Out of the above terms, we select those which produce $\kappa\epsilon^2 \hat{D}w'^2 \bar{w}$. Checking term by term, we find that the following terms may safely be excluded:

- those which include $\boldsymbol{\rho}_2$
- those which included $\mathbf{x}_0^{(1)}$
- those which include $\mathbf{x}_0^{(-1)}$ twice.

The remaining terms are

$$-\epsilon^2 \hat{L}_1 \boldsymbol{\rho}_3^{(1)} - 2\mathbf{n}_2(\mathbf{x}_0^{(-1)}, \boldsymbol{\rho}_4^{(2)}) - \kappa\epsilon^2 \hat{D}\boldsymbol{\rho}_3'^{(1)}. \tag{A27}$$

The first of the above three terms is further dropped because the coupling term included there is linear. The last term is also dropped because the cubic term $\mathbf{n}_3(\mathbf{x}'_0, \mathbf{x}'_0, \mathbf{x}'_0)$ yields neither w nor \bar{w} . Thus, the only relevant term in $\mathbf{b}_5^{(1)}$ is the κ -dependent term in

$$-2\mathbf{n}_2(\mathbf{x}_0^{(-1)}, \boldsymbol{\rho}_4^{(2)}). \tag{A28}$$

The κ -dependent term in $\boldsymbol{\rho}_4^{(2)}$ is

$$(\hat{L}_0 - 2i\omega_0)^{-1}(-\kappa\epsilon^2 \hat{D}\boldsymbol{\rho}_2'^{(2)}). \tag{A29}$$

Because

$$\begin{aligned}\boldsymbol{\rho}_2'^{(2)} &= (\hat{L}_0 - 2i\omega_0)^{-1}(-\mathbf{n}_2(\mathbf{x}_0'^{(1)}, \mathbf{x}_0'^{(1)})) \\ &= -w'^2(\hat{L}_0 - 2i\omega_0)^{-1}\mathbf{n}_2(\mathbf{u}, \mathbf{u}),\end{aligned}\tag{A30}$$

Eq. (A29) becomes

$$\kappa\epsilon^2 w'^2(\hat{L}_0 - 2i\omega_0)^{-1}\hat{D}(\hat{L}_0 - 2i\omega_0)^{-1}\mathbf{n}_2(\mathbf{u}, \mathbf{u}).\tag{A31}$$

Thus, the relevant term in Eq. (A28) is

$$-2\kappa\epsilon^2 w'^2 \bar{w}\mathbf{n}_2(\bar{\mathbf{u}}, (\hat{L}_0 - 2i\omega_0)^{-1}\hat{D}(\hat{L}_0 - 2i\omega_0)^{-1}\mathbf{n}_2(\mathbf{u}, \mathbf{u})),\tag{A32}$$

which yields δ shown in Eq. (21).

Appendix B: Amplitude equation for the Brusselator model

We derive the expression for α, β, γ and δ for the Brusselator model given by Eq.(31). There are three parameters, A , B and d , in Eq.(31). We consider B as a bifurcation parameter while A and d are fixed, so that the expression for α, β, γ and δ will be functions of A and d . Note that such expressions except for δ were already derived in Ref. 1.

The steady solution to Eq. (31) is $(x_0, y_0) = (a, b/a)$. Introducing $\xi = x - x_0$ and $\eta = y - y_0$ and substituting them into Eq. (31), we obtain

$$\frac{d\xi_i}{dt} = (B - 1)\xi_i + A^2\eta_i + f(\xi_i, \eta_i) + \frac{\kappa}{N}\sum_{j=1}^N(\xi_j - \xi_i),\tag{B1a}$$

$$\frac{d\eta_i}{dt} = B\xi_i - A^2\eta_i - f(\xi_i, \eta_i) + \frac{\kappa d}{N}\sum_{j=1}^N(\eta_j - \eta_i),\tag{B1b}$$

where

$$f(\xi, \eta) = \frac{B}{A}\xi^2 + 2A\xi\eta + \xi^2\eta.\tag{B2}$$

In the absence of coupling (i.e., $\kappa = 0$), the trivial solution $(\xi_i, \eta_i) = (0, 0)$ undergoes a supercritical Hopf burcation at $B = B_c \equiv 1 + A^2$. We define the bifurcation parameter as $\epsilon^2 = \frac{B - B_c}{B_c}$. We then obtain

$$\hat{L}_0 = \begin{pmatrix} A^2 & A^2 \\ -(1 + A^2) & -A^2 \end{pmatrix},\tag{B3}$$

$$\hat{L}_1 = (1 + A^2) \begin{pmatrix} 1 & 0 \\ -1 & 0 \end{pmatrix}, \quad (\text{B4})$$

$$\hat{D} = \begin{pmatrix} 1 & 0 \\ 0 & d \end{pmatrix}, \quad (\text{B5})$$

$$\mathbf{u} = \begin{pmatrix} 1 \\ -1 + \mathrm{i}A^{-1} \end{pmatrix}, \quad (\text{B6})$$

$$\mathbf{v} = \frac{1}{2} (1 - \mathrm{i}A \quad -\mathrm{i}A), \quad (\text{B7})$$

$$\omega_0 = A, \quad (\text{B8})$$

$$\hat{L}_0^{-1} = \frac{1}{A^2} \begin{pmatrix} -A^2 & -A^2 \\ A^2 + 1 & A^2 \end{pmatrix}. \quad (\text{B9})$$

$$(\hat{L}_0 - 2\mathrm{i}\omega_0)^{-1} = \frac{1}{3A^2} \begin{pmatrix} A^2 + 2\mathrm{i}a & 3A^2 \\ -A^2 - 1 & -A^2 - 2\mathrm{i}a \end{pmatrix}. \quad (\text{B10})$$

We introduce $\mathbf{u}_i = (\sigma_i, \mu_i)^\text{T}$ ($i = 1, 2, 3$) and write

$$\mathbf{n}_2(\mathbf{u}_1, \mathbf{u}_2) = \left\{ \frac{1 + A^2}{A} \sigma_1 \sigma_2 + A(\sigma_1 \mu_2 + \mu_1 \sigma_1) \right\} \begin{pmatrix} 1 \\ -1 \end{pmatrix}. \quad (\text{B11})$$

$$\mathbf{n}_3(\mathbf{u}_1, \mathbf{u}_2, \mathbf{u}_3) = \frac{\sigma_1 \sigma_2 \mu_3 + \mu_1 \sigma_2 \sigma_3 + \sigma_1 \mu_2 \sigma_3}{3} \begin{pmatrix} 1 \\ -1 \end{pmatrix}. \quad (\text{B12})$$

Substituting these expressions to Eqs. (9)–(11) and (21), we obtain

$$\alpha = \frac{1}{2} + \frac{A^2}{2} \quad (\text{B13})$$

$$\beta = \frac{1}{A^2} + \frac{1}{2} + \mathrm{i} \left(\frac{4}{3A^3} - \frac{7}{3A} + \frac{4A}{3} \right) \quad (\text{B14})$$

$$\gamma = \frac{1}{2} + \frac{d}{2} + \mathrm{i}(-A + Ad) \quad (\text{B15})$$

$$\begin{aligned} \delta = & -\frac{8}{3} + \frac{4}{9A^6} + \frac{8}{3A^4} - \frac{1}{A^3} + \frac{28}{9A^2} + \frac{1}{A} + 2A - \frac{32d}{3} + \frac{4d}{9A^6} - \frac{68d}{9A^2} + \\ & \mathrm{i} \left(2 + \frac{4}{9A^5} + \frac{4}{A^3} + \frac{2}{A^2} + \frac{88}{9A} + \frac{16A}{3} + \frac{14d}{9A^5} + \frac{6d}{A^3} + \frac{20d}{9A} - \frac{16Ad}{3} \right). \end{aligned} \quad (\text{B16})$$

We further obtain

$$c_1 = \frac{\gamma_I}{\gamma_R} = -\frac{A(1-d_y)}{1+d_y}, \quad (\text{B17})$$

$$c_2 = \frac{\beta_I}{\beta_R} = \frac{4-7A^2+4A^4}{3a(2+A^2)}, \quad (\text{B18})$$

$$c_3 = \frac{\delta_I}{\delta_R} = \frac{A(4+5d_y+(2-11d_y)A^2+(d_y-1)A^4)}{4+d_y+(2-10d_y)A^2+(7d_y-2)A^4}, \quad (\text{B19})$$

$$r = \epsilon \sqrt{\frac{\alpha_I}{\alpha_R}} = \epsilon \sqrt{\frac{A^2(1+A^2)}{2+A^2}}. \quad (\text{B20})$$

Using these coefficients, it is straightforward to obtain the expression for the Fourier coefficients a_1, a_2, b_1 and b_2 of Γ .

-
- [1] Y. Kuramoto, *Chemical Oscillations, Waves, and Turbulence* (Springer, New York, 1984).
 - [2] I. Z. Kiss, Y. M. Zhai, and J. L. Hudson, Phys. Rev. Lett. **94**, 248301 (2005).
 - [3] I. Z. Kiss, C. G. Rusin, H. Kori, and J. L. Hudson, Science **316**, 1886 (2007).
 - [4] J. Miyazaki and S. Kinoshita, Phys. Rev. Lett. **96**, 194101 (2006).
 - [5] K. Okuda, Physica D **63**, 424 (1993).
 - [6] D. Hansel, G. Mato, and C. Meunier, Phys. Rev. E **48**, 3470 (1993).
 - [7] H. Kori and Y. Kuramoto, Phys. Rev. E **63**, 046214 (2001).
 - [8] H. Kori, Phys. Rev. E **68**, 021919 (2003).
 - [9] C. Bick, M. Timme, D. Paulikat, D. Rathlev, and P. Ashwin, Phys. Rev. Lett. **107**, 244101 (2011).
 - [10] N. Nakagawa and Y. Kuramoto, Prog. Theor. Phys **89**, 313 (1993).
 - [11] L. Yang, M. Dolnik, A. M. Zhabotinsky, and I. R. Epstein, Phys. Rev. E **62**, 6414 (2000).
 - [12] V. K. Vanag, L. Yang, M. Dolnik, A. M. Zhabotinsky, and I. R. Epstein, Nature **406**, 389 (2000).
 - [13] M. Kim, M. Bertram, M. Pollman, A. von Oertzen, A. S. Mikhailov, H. H. Rotermund, and G. Ertl, Science **292**, 1357 (2001).
 - [14] W. Wang, I. Z. Kiss, and J. L. Hudson, Ind. Eng. Chem. Res. **41**, 330 (2002).
 - [15] H. Kori, C. G. Rusin, I. Z. Kiss, and J. L. Hudson, Chaos **18**, 026111 (2008).
 - [16] H. Varela, C. Beta, A. Bonnefont, and K. Krischer, Phys. Chem. Chem. Phys. **7**, 2429 (2005).

- [17] A. F. Taylor, M. R. Tinsley, F. Wang, and K. Showalter, *Angew. Chem. Int. Edit.* **50**, 10161 (2011).
- [18] I. S. Aranson and L. Kramer, *Rev. Mod. Phys.* **74**, 99 (2002).
- [19] V. García-Morales and K. Krischer, *Contemporary Physics* **53**, 79 (2012).
- [20] J. Guckenheimer and P. Holmes, *Nonlinear Oscillations, Dynamical Systems, and Bifurcations of Vector Fields* (Springer-Verlag, 1983).
- [21] Y. Zhai, I. Z. Kiss, and J. L. Hudson, *Phys. Rev. E* **69**, 026208 (2004).
- [22] Y. Zhai, I. Z. Kiss, H. Daido, and J. L. Hudson, *Physica D: Nonlinear Phenomena* **205**, 57 (2005).
- [23] I. Z. Kiss, Y. M. Zhai, and J. L. Hudson, *Science* **296**, 1676 (2002).